cells

MDPI

Article

Intratumoral Heterogeneity Promotes Collective Cancer Invasion through NOTCH1 Variation

Peter Torab [1], Yue Yan [2], Mona Ahmed [2], Hironobu Yamashita [3], Joshua I. Warrick [3,4], Jay D. Raman [4], David J. DeGraff [3,4,5] and Pak Kin Wong [1,2,4,*]

1 Department of Mechanical Engineering, The Pennsylvania State University, University Park, PA 16802, USA; pot5076@psu.edu
2 Department of Biomedical Engineering, The Pennsylvania State University, University Park, PA 16802, USA; yby5024@psu.edu (Y.Y.); maa6782@psu.edu (M.A.)
3 Department of Pathology and Laboratory Medicine, The Pennsylvania State University, Hershey, PA 17033, USA; hyamashita@pennstatehealth.psu.edu (H.Y.); jwarrick@pennstatehealth.psu.edu (J.I.W.); ddegraff@pennstatehealth.psu.edu (D.J.D.)
4 Penn State Health Milton S., Hershey Medical Center, Department of Surgery, Hershey, PA 17033, USA; jraman@pennstatehealth.psu.edu
5 Department of Biochemistry and Molecular Biology, The Pennsylvania State University, Hershey, PA 17033, USA
* Correspondence: pak@engr.psu.edu

Abstract: Cellular and molecular heterogeneity within tumors has long been associated with the progression of cancer to an aggressive phenotype and a poor prognosis. However, how such intratumoral heterogeneity contributes to the invasiveness of cancer is largely unknown. Here, using a tumor bioengineering approach, we investigate the interaction between molecular subtypes within bladder microtumors and the corresponding effects on their invasiveness. Our results reveal heterogeneous microtumors formed by multiple molecular subtypes possess enhanced invasiveness compared to individual cells, even when both cells are not invasive individually. To examine the molecular mechanism of intratumoral heterogeneity mediated invasiveness, live single cell biosensing, RNA interference, and CRISPR-Cas9 gene editing approaches were applied to investigate and control the composition of the microtumors. An agent-based computational model was also developed to evaluate the influence of NOTCH1 variation on DLL4 expression within a microtumor. The data indicate that intratumoral variation in NOTCH1 expression can lead to upregulation of DLL4 expression within the microtumor and enhancement of microtumor invasiveness. Overall, our results reveal a novel mechanism of heterogeneity mediated invasiveness through intratumoral variation of gene expression.

Keywords: single cell analysis; tumor subtypes; basal; luminal; tumor-on-chip; biosensing

Citation: Torab, P.; Yan, Y.; Ahmed, M.; Yamashita, H.; Warrick, J.I.; Raman, J.D.; DeGraff, D.J.; Wong, P.K. Intratumoral Heterogeneity Promotes Collective Cancer Invasion through NOTCH1 Variation. *Cells* **2021**, *10*, 3084. https://doi.org/10.3390/cells10113084

Academic Editors: Tuhin Subhra Santra and Fan-Gang Tseng

Received: 26 July 2021
Accepted: 8 November 2021
Published: 9 November 2021

1. Introduction

In the United States, bladder cancer is a common malignancy, with an estimated 83,730 people diagnosed and over 17,200 individuals dying annually [1]. At both the cellular and molecular levels, bladder cancer is an extraordinarily heterogeneous disease. At the individual patient level, several groups have independently completed molecular characterization of human bladder cancer [2–4]. These efforts led to the discovery of luminal, basal/squamous, and other transcriptional subtypes (stroma-rich and neuroendocrine-like) of the muscle-invasive bladder cancer [5]. Luminal bladder cancer (so called because of expression of luminal urothelial markers) is often associated with histology consistent with urothelial cell carcinoma and can be further classified into luminal papillary, luminal non-specified, and luminal unstable (luminal papillary is the most common molecular subtype). Luminal cancer cells are controlled by the transcriptional master regulators, such as FOXA1, PPARγ, and GATA3 [6,7]. Luminal cancer cells are reportedly chemoresistant [3],

while a subset of these tumors appear to respond favorably to immune checkpoint blockade [8]. On the other hand, the basal/squamous subtype of bladder cancer is enriched for morphologic squamous differentiation. Such basal/squamous bladder cancers are highly lethal [3]. Basal/squamous cancer cells are typically classified by elevated expression of specific cytokeratins, such as KRT5 and KRT14 [6]. While it appears that basal/squamous tumors respond favorably to neoadjuvant, platinum-based chemo-therapy and targeted therapeutic approaches, recent reports indicate patients with basal/squamous bladder cancer have inferior overall and disease-specific survival rates [3].

While associations between transcriptional subtypes and clinical outcome have been observed at the patient level, the impact of intratumoral heterogeneity is similarly associated with aggressive disease characteristics. For example, tumors with intratumoral cellular heterogeneity usually present at advanced stage and exhibit poor clinical outcome [9]. Relative to pure urothelial cell carcinoma, urothelial carcinoma with squamous differentiation often presents as high-stage disease with lymph node metastasis [10,11]. It has been suggested that distinct cell subpopulations may cooperate as a community to support cancer progression [12]. For example, cancer cells with invasive characteristics can promote the invasion of non-invasive epithelial cells in a co-culture spheroid model of breast and prostate cancer [13]. Basal cancer cells can serve as invasive leader cells to promote collective invasion of breast cancer [14,15]. Furthermore, NOTCH1, which sup-presses basal phenotypes and bladder cancer progression [16–18], negatively regulates the formation of a DLL4 expressing subpopulation that promotes collective cancer invasion [19–21]. In a 3D invasion model of bladder cancer, microtumors with a high level of DLL4 at the invasive front exhibited enhanced invasiveness [22]. Overall, the available evidence suggests non-cell autonomous interactions between heterogeneous cell populations can enhance the aggressiveness of cancer and underscores heterogeneous cell populations may collectively promote cancer invasion. Nevertheless, the influence of intratumoral heterogeneity on bladder cancer cell behavior remains poorly understood, limiting innovation in the clinical management of this common disease.

In this study, we investigate the influence of tumor heterogeneity on the invasiveness of cancer by establishing a tumor bioengineering approach (Figure 1a,b). The tumor bioengineering approach simultaneously generates a large number of microtumors in a single assay and recapitulates the important features of the tumor microenvironment, including multilayer extracellular matrix (ECM) components and heterogeneous molecular subtypes of cancer cells. In addition, we incorporate a locked nucleic acid (LNA) single cell biosensor to perform in situ gene expression analysis in 3D microtumors. Using established cell lines with luminal and basal/squamous signatures, transient knockdown by siRNA, CRISPR knockout, and in silico models, we examine the influence of heterogeneity of NOTCH1-DLL4 signaling on bladder cancer invasion. The results suggested that variation, or molecular heterogeneity, of NOTCH1 expression within the microtumor can promote the invasiveness of heterogeneous bladder cancer. Overall, our tumor bioengineering approach reveals a novel mechanism of heterogeneity-mediated invasiveness in bladder cancer.

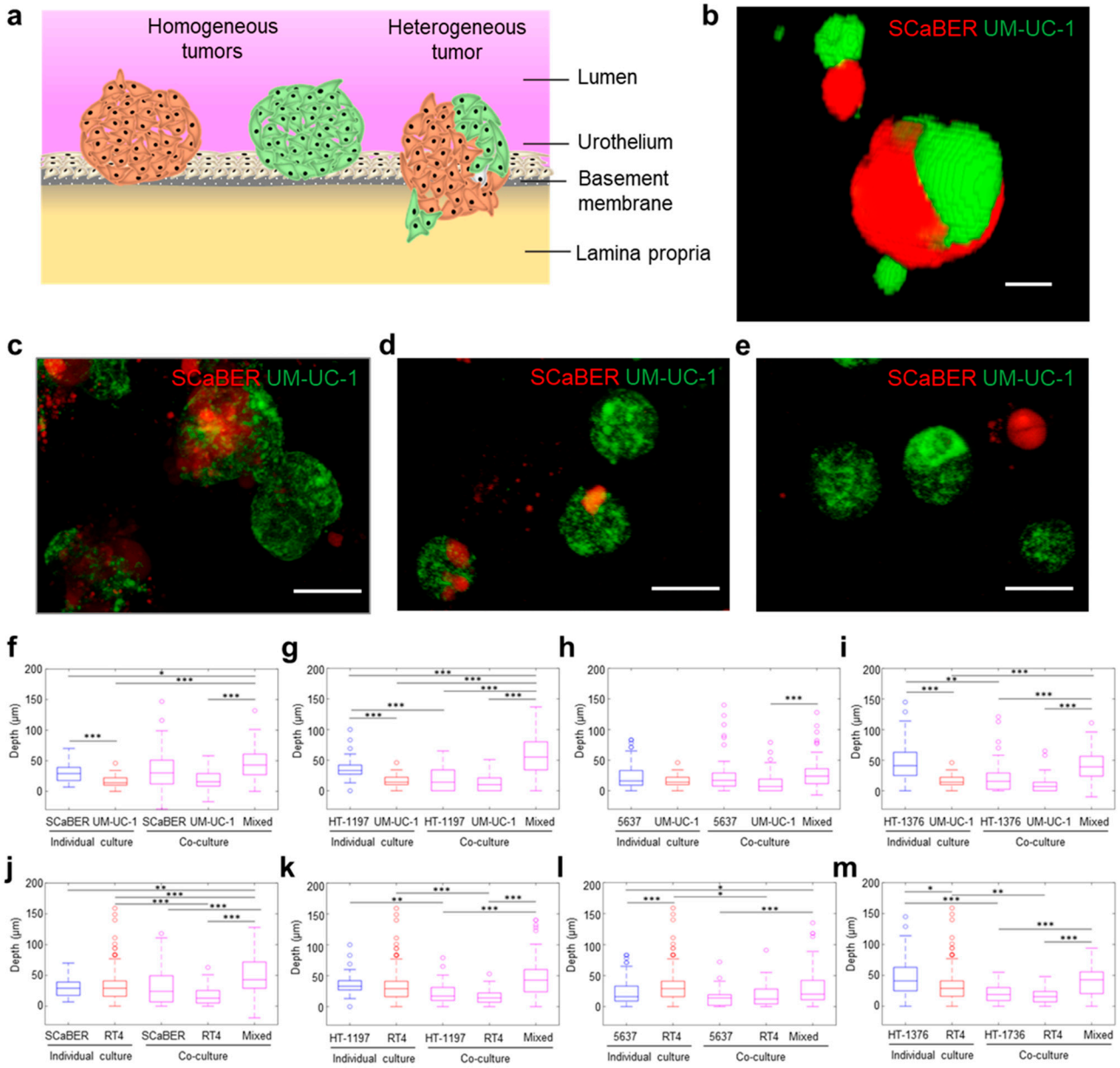

Figure 1. Co-culture microtumors invading extracellular matrix model. (**a**) Schematic of heterogeneous microtumor invasion through basement membrane and lamina propria. (**b**) Three-dimensional (3D) reconstruction of heterogeneous microtumor (side vide) created using NIH ImageJ 3D viewer plugin. Scale bar, 10 μm. (**c**–**e**) Vertical projection views of SCaBER-UM-UC-1 co-culture. Scale bars, 50 μm. (**f**–**m**) Invasion depth into Matrigel for basal- (blue) and luminal-type (red) microtumors, as well as co-culture (purple) microtumors. Co-culture results are separated for homogeneous and heterogeneous (mixed) microtumors within co-culture experiments (* $p < 0.05$, ** $p < 0.01$, *** $p < 0.001$ Kruskal–Wallis ANOVA test with Tukey–Kramer post hoc test).

2. Materials and Methods

2.1. Single Layer Invasion Model

In this study, two 3D invasion models were used. A simplified tissue model representing the basement membrane matrix was used to screen bladder cancer cell lines for their ability to penetrate the basement membrane [22]. In particular, a self-assembly process was used to generate a large number of bladder cancer microtumors on top of a layer of matrix representing the basement membrane composition. Briefly, growth factor reduced Matrigel (Corning, Corning, NY, USA) was diluted to 8 mg/mL in chilled, complete culture medium (Corning, Corning, NY, USA). Fluorescent beads (Spherotech, Lake Forest, IL, USA) were

then added at a volume ratio of 1:10,000 to label the Matrigel for imaging. An amount of 40 µL labeled Matrigel was applied to each well of a chilled glass-bottom 96-well plate (CellVis, Mountain View, CA, USA), which was then placed in a humidified cell incubator at 37 °C, 5% CO_2 for 30 min to solidify. Cells were then detached using 0.25% trypsin, 0.53 mM EDTA solution (Corning, Corning, NY, USA), suspended in complete culture medium at a concentration of 10^6 cells/mL, and seeded atop the solidified Matrigel at a concentration of 10^4 cells per well. The plate was then covered and returned to the cell culture incubator for 3 days before imaging.

2.2. Multilayer Invasion Model

A multilayer tissue model representing the basement membrane (Matrigel) and lamina propria (collagen type I) ECM layers was developed to study microtumor invasion for cell lines and combinations of cell lines that showed a high potential for invasion in the simplified model. Collagen type I from rat tail (SigmaAldrich, St. Louis, MO, USA) at a starting concentration of 4 mg/mL was diluted to 2 mg/mL in complete culture medium (Corning, Corning, NY, USA), and neutralized using 1M NaOH to a final pH of 7.5. Collagen concentrations ranging from 2.0 to 2.5 mg/mL were tested experimentally, and a concentration of 2.0 mg/mL was found to reliably produce a uniform solid gel layer within 60 min. The pH was adjusted to 7.5 using NaOH, allowing for fast gelation and physiological pH [23]. The final concentration of FBS (Corning, Corning, NY, USA) was 20%. 40 µL of collagen was added to each well of a chilled glass-bottom 96-well plate (CellVis, Mountain View, CA, USA), which was then placed in a humidified cell incubator at 37 °C, 5% CO_2 for 60 min to solidify. A gelation temperature of 37 °C was chosen to produce a small, uniform pore size in the gel [23–25]. Solidification was confirmed by visually inspecting for turbidity. After collagen gelation, a thin layer of Matrigel was loaded on top of the collagen similar to the single layer invasion model. Growth factor reduced Matrigel (Corning, Corning, NY, USA) was diluted to 5 mg/mL in chilled, complete culture medium (Corning, Corning, NY, USA). Fluorescent beads (Spherotech, Lake Forest, IL, USA) were then added at a volume ratio of 1:10,000 to label the Matrigel for imaging. An amount of 10 µL labeled Matrigel was then carefully applied to each well on top of the solidified collagen I layer, and the entire 96-well plate was then returned to the cell incubator for 15 min to solidify. The Matrigel layer is thicker compared to the bladder basement membrane for uniform coverage and visualization of the microtumor invasiveness. Cells were detached using 0.25% trypsin, 0.53 mM EDTA solution, and suspended in complete culture medium at a concentration of 10^6 cells/mL, then seeded atop the solidified Matrigel layer at a concentration of 10^4 cells per well.

2.3. Cell Culture

The bladder cancer cell lines RT4, UM-UC-3, SCaBER, HT-1197, HT-1376, and 5637 were obtained from ATCC, and UM-UC-1 was obtained from Sigma-Aldrich. RT4 cells were maintained in McCoy's 5A culture medium and all other cell lines were maintained in MEM with 2 mM glutamine (Corning, Corning, NY, USA). Culture medium for HT-1197 and HT-1376 was supplemented with 1× non-essential amino acids and 1 mM sodium pyruvate (Gibco, Waltham, MA, USA). All culture media were supplemented with 10% fetal bovine serum (Corning, Corning, NY, USA) and 1 µg/mL Gentamicin (Gibco, Waltham, MA, USA). Cells were grown in 60 mm tissue culture dishes and were incubated at 37 °C, 5% CO_2 with 95% humidity. The cells were examined under a microscope on a daily basis, and the medium was renewed every 2 days. Cells were passaged at 70% confluence using 0.25% trypsin, 0.53 mM EDTA solution (Corning, Corning, NY, USA).

2.4. Cell Treatments

DLL4 siRNA, NOTCH1 siRNA, and non-targeting control siRNA were purchased from Santa Cruz Biotech (Dallas, TX, USA). These siRNAs were tested and optimized in previous studies [22,26,27]. The designs, however, did not rule potential off-target

effects. Transfection was performed in monolayer culture using Hiperfect transfection reagent (Qiagen, Germantown, MD, USA) with an siRNA concentration of 30 nM for 24 h prior to microtumor self-assembly. LNA fluorescent probes (Integrated DNA Technologies, Coralville, IA, USA) targeting DLL4 and NOTCH1 were attached to MUTAB-coated GNRs (Nanopartz, Loveland, CO, USA) in Tris-EDTA buffer to form GNR-LNA biosensor complex. Cells were incubated with the biosensor for 12 h to allow for sufficient uptake. Cells were stained using CellTracker Green CMFDA or Red CMTPX (Invitrogen, Carlsbad, CA, USA) at a concentration of 20 μM in PBS for 30 min. Stains were alternated in experimental replicates.

2.5. Computational Model

An agent-based computational model was developed for evaluating the effects of intratumoral variations of NOTCH1 expression. The numerical model was developed based on reported studies of NOTCH lateral inhibition [19,28]. The model consisted of either 8 by 8 or 16 by 16 discretized elements (agents) to represent the microtumor and was solved in MATLAB or Octave. Parameters of the basic model were obtained from the previous study and were adjusted as indicated to evaluate the effects of NOTCH1 and DLL4 variations [28]. A periodic boundary condition was applied to the microtumor. Cells surrounding the first and second layers of a cell were considered in contact due to the dynamic filopodial activity of the cells [28]. The numerical experiment was performed until an equilibrium pattern was formed. All numerical results are representatives of at least five independent simulations.

2.6. CRISPR Knockout

UM-UC-1 cells (2×10^5) cells were transfected with 2.5 μg of HNF-3alpha CRISPR/Cas9 KO plasmid (Santa Cruz; sc-400743) using Lipofectamine 3000 (Thermo Fisher Scientific, Waltham, MA, USA). After 48 h, transfected cells were trypsinized and resuspended in PBS. Three GFP-positive cells were isolated via flow cytometry into single wells of 96-well plates (Corning, Corning, NY, USA) in 100 μL aliquots. Sorted cells were expanded and sequentially transferred to 24-well, 6-well dishes and T75 flasks (Corning, Corning, NY, USA). Finally, FOXA1 knockout was confirmed by qPCR and western blotting analysis.

2.7. Statistics and Data Analysis

Invasion depth measurements (Figure 1f–m) with unequal sample sizes were compared using a Kruskal–Wallis one-way ANOVA on ranks followed by a Tukey–Kramer post hoc test. Biosensor intensity (Figure 3b,c) measurements were compared using one-way ANOVA followed by Tukey's HSD post hoc test. Median invasion depth of co-culture microtumors was compared to that of each individual comprising cell line using a one-tailed Wilcoxon rank-sum test. To define a threshold for the invasive fraction, the K-means clustering algorithm (k = 2) is applied. Distributions of invasive fraction were compared using the Chi-square test. Statistical analysis was performed using the MATLAB statistics toolbox (Mathworks, Natick, MA, USA). For all figures, NS $p > 0.05$, * $p < 0.05$, ** $p < 0.01$, *** $p < 0.001$, and **** $p < 0.0001$.

3. Results

3.1. Cellular Heterogeneity Enhances Invasiveness of Bladder Microtumors

The presence of multiple histologic variants within a bladder cancer tumor is common, and molecular heterogeneity is often observed when multiple variants are present [11]. To study these effects, cell lines representing two most common bladder cancer subtypes, i.e., luminal papillary and basal/squamous, were co-cultured to form mixed (i.e., heterogeneous) microtumors [5]. The single layer invasion model consisting of simulated basal membrane matrix was first applied to test cell lines representing the luminal papillary subtype (UM-UC-1, RT4) and basal/squamous subtype (SCaBER, HT-1197, HT-1376, 5637) individually and in every possible basal-luminal combination (Supplementary Table S1).

The cells were self-assembled on the ECM mimicking gel and formed 3D microtumors 20–50 μm in diameter (Supplementary Movies S1–S3). For co-culture experiments, cell lines were stained separately, then mixed at a 1:1 ratio (Figure 1b). Within mixed microtumors, individual cell types tended to aggregate together (Figure 1c). Microtumors composed of both cell types (mixed or heterogeneous) and a single cell type (homogeneous) were observed in the co-culture experiment (Figure 1d,e).

Microtumors invaded into the ECM-mimicking gel in the experiment (Figure 1f–m). In accordance with our previous report [22], the invasion depth correlated the invasiveness of the cancer cell lines determined by animal models and other 3D invasion assays [29–32]. For example, non-invasive cell lines, such as UM-UC-1 (derived from grade 2 bladder cancer and classified as the luminal papillary subtype based on the consensus molecular classification of muscle-invasive bladder cancer) [5,32], produced microtumors that displayed only slight deformation of the matrix. The depth of deformation is typically less than 50 μm and can be understood by contact mechanics [33]. In contrast, invasive cell lines, such as HT-1376 (derived from grade 3 bladder cancer with a basal/squamous signature based on the consensus molecular classification of muscle-invasive bladder cancer), displayed a relatively high invasiveness as indicated by the invasion depth [5,34].

Heterogeneity in invasiveness among microtumors has been reported in organoid invasion models [35]. Similarly, we observed only a portion of microtumors penetrated the gel despite the microtumors were formed by a single cell line. We, therefore, characterized the fraction of microtumors which invaded into the gel. In this study, the invasive fraction is defined by the portion of microtumors with an invasion depth over 50 μm. This threshold value is consistent with our previous study [22], and a similar threshold value was also obtained by clustering analysis (Supplementary Figure S1a,b). The invasive fraction showed a similar trend compared to the invasive depth (Supplementary Figure S1c). In particular, UM-UC-1 had no (0%) invasive fraction while HT-1376 had a high fraction (~30%) of invasive microtumors. Notably, most cell lines exhibited a small fraction (5–10%) of invasive microtumors despite having a low level of median invasion depth, suggesting heterogeneity within individual cell lines.

We examined the influence of combining luminal–basal cells on the invasiveness of microtumors (Figure 1f–m, Figures S2 and S3). We observed an increase in invasiveness in microtumors with mixed luminal and basal cell types compared to homogenous microtumors formed by individual cell lines. The median invasion depth of mixed microtumors was larger than most homogeneous microtumors (Figure 1f–m). There was a significant increase (one-tailed Wilcoxon rank sum test) in the median invasion depth of mixed microtumors compared to the majority of basal cell lines (75%) and luminal cell lines (88%) that comprised the mixed microtumors. For instance, despite co-culture only had a small effect on the dimension of the microtumors, both the invasion depth and the invasive fraction of mixed SCaBER/UM-UC-1 microtumors were significantly enhanced compared to SCaBER and UM-UC-1 cells cultured individually (Supplementary Figures S4 and S5). For invasive cells, such as HT-1376, similar or slightly higher invasion depths and invasive fraction were observed when mixed with UM-UC-1 or RT4, which were less invasive individually. We also analyzed the influence of the microtumor composition on the invasiveness as both homogeneous and heterogeneous microtumors were formed in the co-culture experiments. Heterogeneous microtumors showed a larger invasion depth compared to most homogeneous microtumors in co-culture experiments (Figure 1f–m). Since both basal and luminal cells were in the same well, the enhancement in invasiveness could not be fully explained by diffusible factors and was likely contributed by a contact dependent mechanism. Taken together, these results support the notion that the presence of heterogeneous subtypes enhances bladder cancer invasion via a contact-dependent mechanism.

3.2. Heterogeneous Microtumors Efficiently Invade Matrices Found in the Bladder Wall

We further evaluated the behaviors of mixed microtumors by establishing a multilayer invasion model. The materials and gelation procedures were optimized to create a microen-

vironment that mimics the basement membrane and lamina propria [23–25]. Furthermore, the multilayer model allowed the generation of a gradient of serum or other chemicals for promoting directional invasion of microtumors. In this study, a gradient of fetal bovine serum (FBS) was created across the layers to simulate a nutrient gradient in the bladder wall. Similar to the single layer invasion model, microtumors were formed and allowed to invade into the matrices (Figure 2a). The use of the multilayer invasion model can reveal the microtumor's ability to breach the ECM protein found in the basement membrane and the underlying lamina propria (Figure 2b). The ability of cells to progress through both of these layers would indicate that the tumor has a higher chance to progress into muscle invasive bladder cancer, while non-muscle invasive tumors would not be expected to penetrate through the ECM mimicking gel.

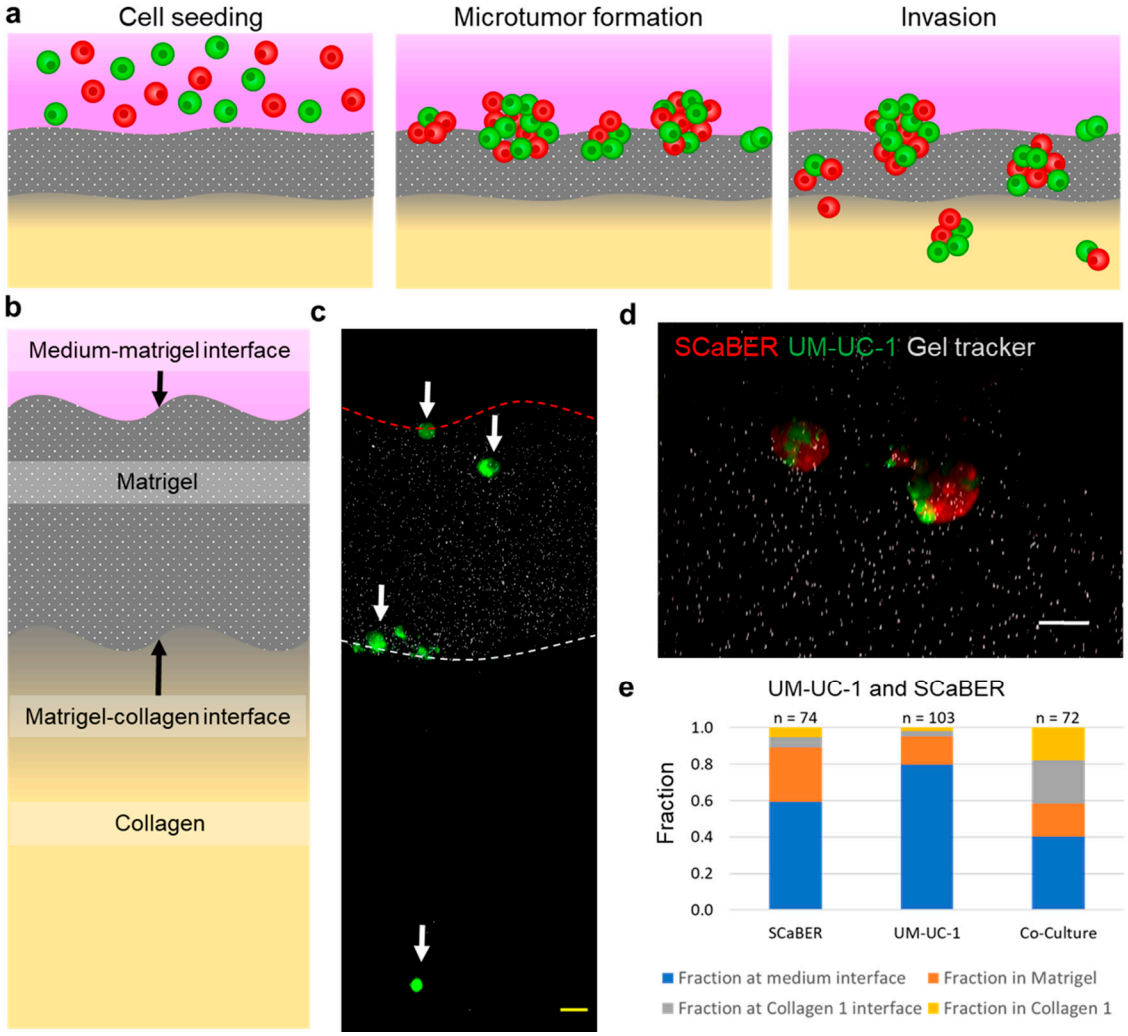

Figure 2. Heterogeneous microtumors invading multilayer ECM. (**a**) Schematics of microtumor formation and invasion of heterogeneous microtumors. (**b**) Schematic of multilayer ECM model. (**c**) Cross-section view of multilayer ECM. White arrows indicate microtumors in each of the four regions. Red dotted line indicates the medium–Matrigel interact, and white dotted line indicates the Matrigel–collagen interface. (**d**) Heterogeneous microtumor invading the Matrigel layer. Scale bars, 50 μm. (**e**) Fraction of microtumors counted in each region on the multilayer invasion model. Results represent the total from 6 independent experiments (see Supplementary Table S2).

In the experiment, the cells formed microtumors in a manner similar to the single layer invasion model and invaded into different regions of the gel layers, becoming embedded at the interfaces between layers or within the gel layers (Figure 2c,d). UM-UC-1 and SCaBER were chosen for further investigation due to their molecular signatures (Supplementary

Table S1) and synergy in microtumor invasiveness. For homogeneous culture, SCaBER and UM-UC-1 did not display a high invasiveness, and the majority of microtumors stayed at the medium–Matrigel interface or embedded within the Matrigel (Figure 2e). Only a very small fraction (less than 5%) of microtumors were able to reach the collagen layer. In contrast, co-culture microtumors exhibited an enhanced capability of invading into the matrices (Supplementary Table S2). Some mixed microtumors (~20%) penetrated through the Matrigel layer and reached the Matrigel–collagen interface. Furthermore, a substantial fraction (~20%) reached into the collagen layer, suggesting an ability to invade through both Matrigel and collagen. These observations further support the notion that heterogeneous microtumors possess enhanced invasiveness.

3.3. NOTCH1-DLL4 Signaling in Invasive Microtumors

We investigated the mechanism that drives the enhanced invasiveness of mixed microtumors. In particular, we studied the role of NOTCH signaling, which mediates contact-dependent signaling between cells and regulates bladder cancer invasiveness [22]. We first evaluated the expressions of NOTCH1 and DLL4 in UM-UC-1 and SCaBER microtumors using a live single cell biosensor, which was demonstrated in cancer cells, tumor organoids derived from patients, and tumor tissues (Supplementary Figure S6) [22,36,37]. The cells were then seeded into the multilayer invasion model and imaged after 72 h to measure the target mRNA expression (Figure 3a). Figure 3b,c show the average intensities of SCaBER, UM-UC-1, and mixed microtumors. UM-UC-1 expressed a high level of NOTCH1 mRNA relative to SCaBER, which was barely detectable. In mixed microtumors, the average NOTCH1 expression showed an intermediate value between the expression values for individual cell lines. Notably, a large variation of NOTCH1 mRNA expression was observed within the microtumor. Some cells in the microtumor displayed a high level of NOTCH1 expression while some cells had no detectable NOTCH1 expression (Figure 3a). This observation was not surprising as UM-UC-1 and SCaBER expressed high and low levels of NOTCH1, respectively. In contrast, while not significant (p-value = 0.181), the expression of DLL4 mRNA was highest in the co-culture case. This observation was interesting as the expression of DLL4 in co-culture microtumors was anticipated to be in between the two cell lines.

To test whether the enhanced invasiveness of mixed tumors is associated with NOTCH1-DLL4 signaling, NOTCH1 and DLL4 siRNA were applied in either UM-UC-1, SCaBER, or both cell types (Figure 4a,b and Supplementary Figure S7). Cells were each alternately treated with NOTCH1, DLL4, and non-targeting (control) siRNA before self-assembly. In the experiment, siRNA inhibition of DLL4 in individual cell lines and in both cell lines in co-culture substantially inhibited the cells' ability to invade through the Matrigel layer (Figure 4c and Supplementary Table S3). DLL4 siRNA reduced invasion when applied to either cell line or both cell lines with similar efficiency. Most microtumors stayed at the medium–Matrigel interface or in the Matrigel, and no cells were able to reach into the collagen layer (i.e., 0%). This observation is consistent with the view that DLL4 supports collective cancer invasion [19–22]. On the other hand, NOTCH1 transient knockdown was performed on individual cell line or both cell lines in the co-culture invasion assay (Figure 4d). When applied to either cell line, which created diverse NOTCH1 expression within the microtumor, NOTCH1 knockdown resulted in an increase in invasiveness compared to control (Supplementary Table S4). The fraction of microtumor reaching the collagen layer increased for NOTCH1 knockdown in either cell line (~30%). No microtumors were observed to stay at the Matrigel–collagen interface. The fraction of microtumors in collagen was higher than co-culture without transient knockdown (~20%). Interestingly, inhibition of NOTCH1 in both UM-UC-1 and SCaBER, which attenuated the overall NOTCH1 expression in the microtumor, did not enhance the fraction invaded into collagen (Supplementary Table S4), which essentially eliminated the co-culture-enhanced invasiveness. Some of the microtumors were trapped at the Matrigel–collagen interface. Together, NOTCH1-DLL4 signaling is associated with the ability of microtumor to penetrate

through collagen, and the enhanced invasiveness of mixed tumors correlated with the variation of NOTCH1 expression within the microtumor.

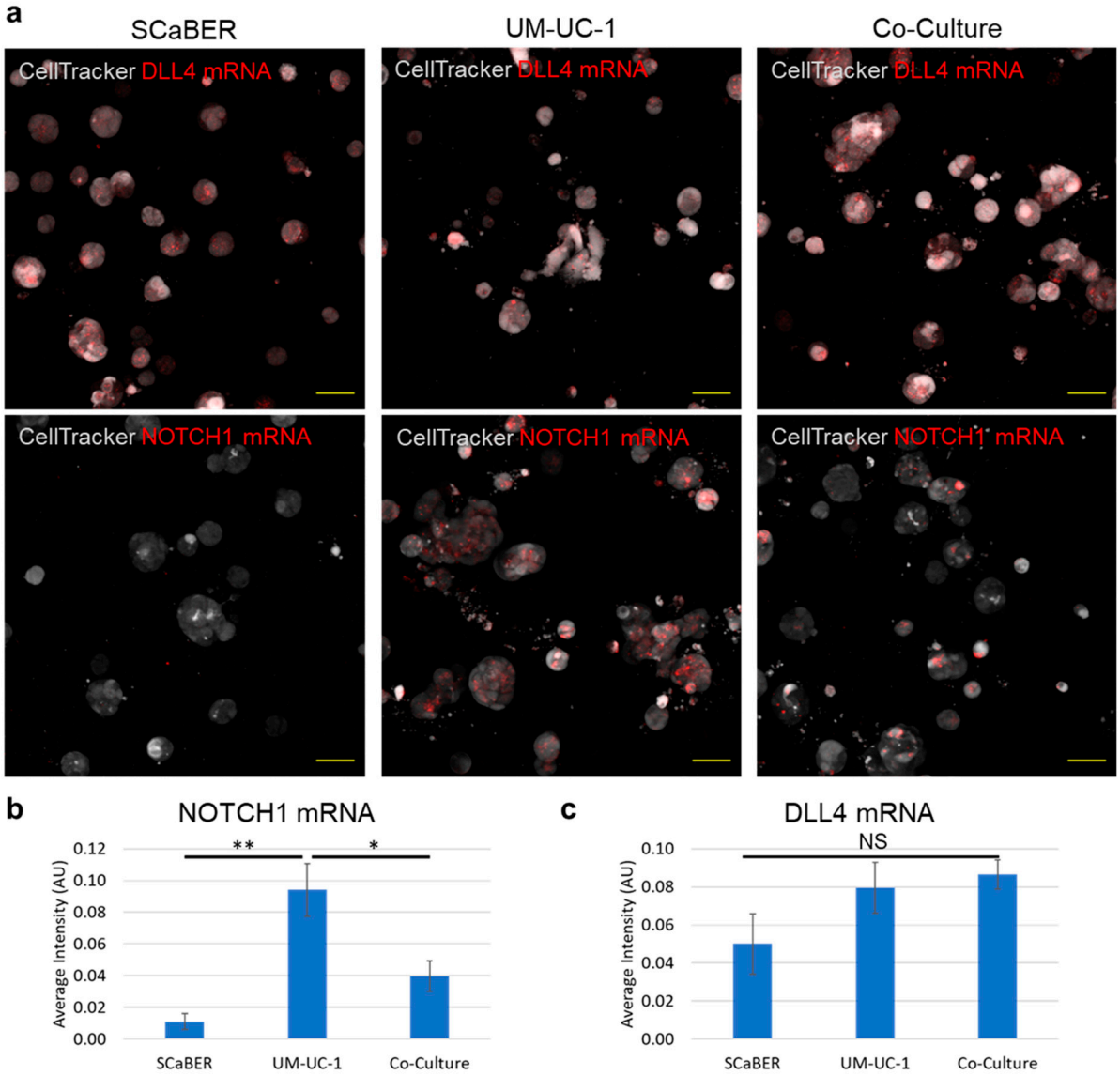

Figure 3. Detection of NOTCH1 and DLL4 mRNA expressions and variations using the GNR-LNA biosensor. (**a**) Representative images of biosensors in SCaBER, UM-UC-1, and co-culture microtumors. Scale bars, 50 µm. (**b**,**c**) Fluorescence intensity of (**b**) NOTCH1 and (**c**) DLL4 biosensors. Results are representative of three independent experiments. Data represent mean ± SEM (NS $p > 0.05$, * $p < 0.05$, ** $p < 0.01$, One-way ANOVA test with Tukey's post hoc test).

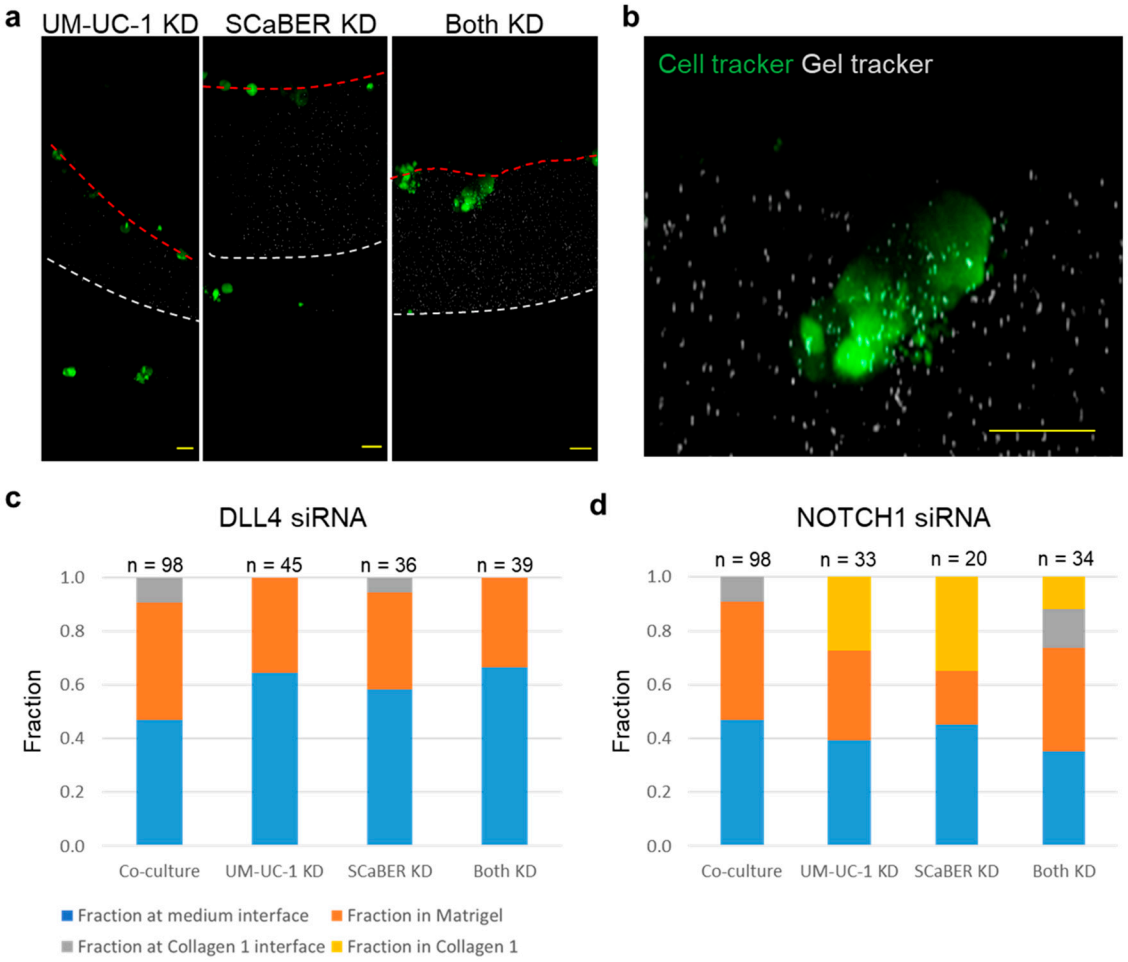

Figure 4. RNA interference applied to DLL4 and NOTCH1. (**a**) Representative images of microtumors treated with NOTCH1 siRNA. (**b**) Detail view of invasive microtumor. Scale bars, 50 µm. (**c**,**d**) Fraction of microtumors counted in each region with (**c**) DLL4 siRNA and (**d**) NOTCH1 siRNA. Co-culture represents UM-UC-1 and SCaBER treated with control siRNA. Results represent the totals from three independent experiments (see Supplementary Tables S3 and S4).

3.4. UM-UC1- and UM-UC-1 FOXA1 KO Co-Culture Promotes Microtumor Invasion

The influences of luminal-basal co-culture and NOTHC1 variation on microtumor invasiveness were further investigated by CRISPR-Cas9 gene editing. FOXA1 is an emerging regulator of the luminal subtype of bladder cancer, and FOXA1 overexpression can drive basal bladder cancer cells to assume a more luminal phenotype [6,38]. FOXA1 has also been implicated in the regulation of NOTCH1 in other cancer types [39]. A FOXA1 knockout (KO) cell line was generated from the luminal UM-UC-1 cell line using CRISPR-Cas9 gene editing. The UM-UC-1 FOXA1-KO cell line exhibited a reduced expression of NOTCH1 and NOTCH1 targeted genes, such as HEY1, HES1, and CDKN1A (p21) compared to the wild-type cell (Figure 5a). The invasiveness of the UM-UC-1 FOXA1 KO cells was tested in the multilayer invasion model (Figure 5b). The KO cells showed only a slight increase in the fraction of microtumor reaching the collagen interface while the overall invasive fraction was similar between the wild-type and FOXA-KO UM-UC-1 cells (Supplementary Table S5). In other words, FOXA1 KO individually only had a weak effect on the invasiveness of the microtumor. Intriguingly, UM-UC-1 FOXA1-KO and UM-UC-1 wild type co-culture, which created diverse FOXA1 and NOTCH1 expressions within the microtumor, was much more invasive than microtumors formed by wild-type or KO cells individually (Supplementary Table S5). Both the overall invasive fraction and the fraction of microtumor invaded into collagen increased by co-culture of the cells. Furthermore, the mixed microtumors were less likely to be trapped at the Matrigel–collagen interface. These results further support

the notion that variation (instead of the average value) of NOTCH1 expression within the microtumor promotes the invasiveness of microtumors.

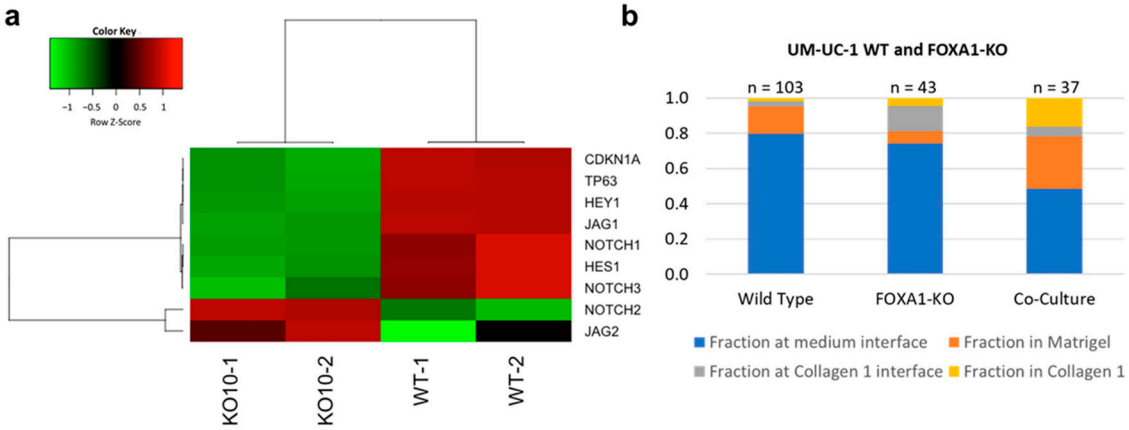

Figure 5. FOXA1 and NOTCH1 expression. (**a**) RNA-seq results indicate that NOTCH1 is downregulated in FOXA1 knockout UM-UC-1 cells. (**b**) Number of microtumors in each region for UM-UC-1 wild type, FOXA1 knockout, and co-culture conditions (see Supplementary Table S5).

3.5. Computational Modeling of Mixed Microtumor with Variations in NOTCH1 Expression

To evaluate how NOTCH1 variation may contribute to the enhanced invasiveness, we developed an agent-based computational model for evaluating the effects of NOTCH1 expression variations within the microtumor. The agent-based model considered the production, degradation, and cis-inhibition of NOTCH1 and DLL4 [40]. The production rate of NOTCH1 was promoted by the level of DLL4 of cells in contact, and the production rate of DLL4 was attenuated by the NOTCH1 activity (Figure 6a). These interactions resulted in lateral inhibition of DLL4 expressing cells. When the maximum production rate of NOTCH1, R_N, was uniform for all cells, lateral inhibition of NOTCH1-DLL4 created a pattern with regular spacing of DLL4 expressing cells surrounded by NOTCH1 expressing cells (Figure 6b). The check box (or mosaic) pattern formed with various values of maximum NOTCH1 and DLL4 production rates (Supplementary Figure S8). Lateral inhibition provides a robust mechanism for the formation of the checker box pattern, which is used to explain hair cell patterning during embryonic development [41].

Using the agent-based model, we investigated the effect of intratumoral NOTCH1 expression variations. By introducing some variation of NOTCH1 production rate, the checker box pattern was disrupted (Supplementary Figure S9b). Unlike the checker box pattern with DLL4 expressing cells surrounded by NOTCH1 expressing cells, clusters of DLL4 expressing cells and NOTCH1 expressing cells were formed and occupied in alternative regions. Examining the expression dynamics revealed that the cells committed into either NOTCH1 or DLL4 phenotypes with various equilibrium values (Supplementary Figure S9b). These observations suggest variation of NOTCH1 expression can have a significant effect on DLL4 activities. To understand the effect of intratumoral variation of NOTCH1 expression, we systematically adjusted the level of average NOTCH1 production rate and NOTCH1 production rate variation among the cells (Figures 6c and S9c). With a high level of average NOTCH1 production rate, the checker box pattern was formed in most cases. Remarkably, a variation of the maximum NOTCH1 production rate was sufficient to modulate the checker box pattern to DLL4 clusters, despite that the average value was maintained constant. The level of variation of NOTCH1 expression increased with the cluster size. In addition, the NOTCH1 variation required for inducing the transition from checker box pattern to DLL4 clusters increased with the average NOTCH production rate (Figure 6c). Even at a high average NOTCH1 production rate, a sufficiently large variation could disrupt the checker box pattern and created DLL4 clusters. The agent-based model

suggests that intratumoral variation of NOTCH1 expression can contribute to the formation of DLL4 expressing cell clusters in the microtumors.

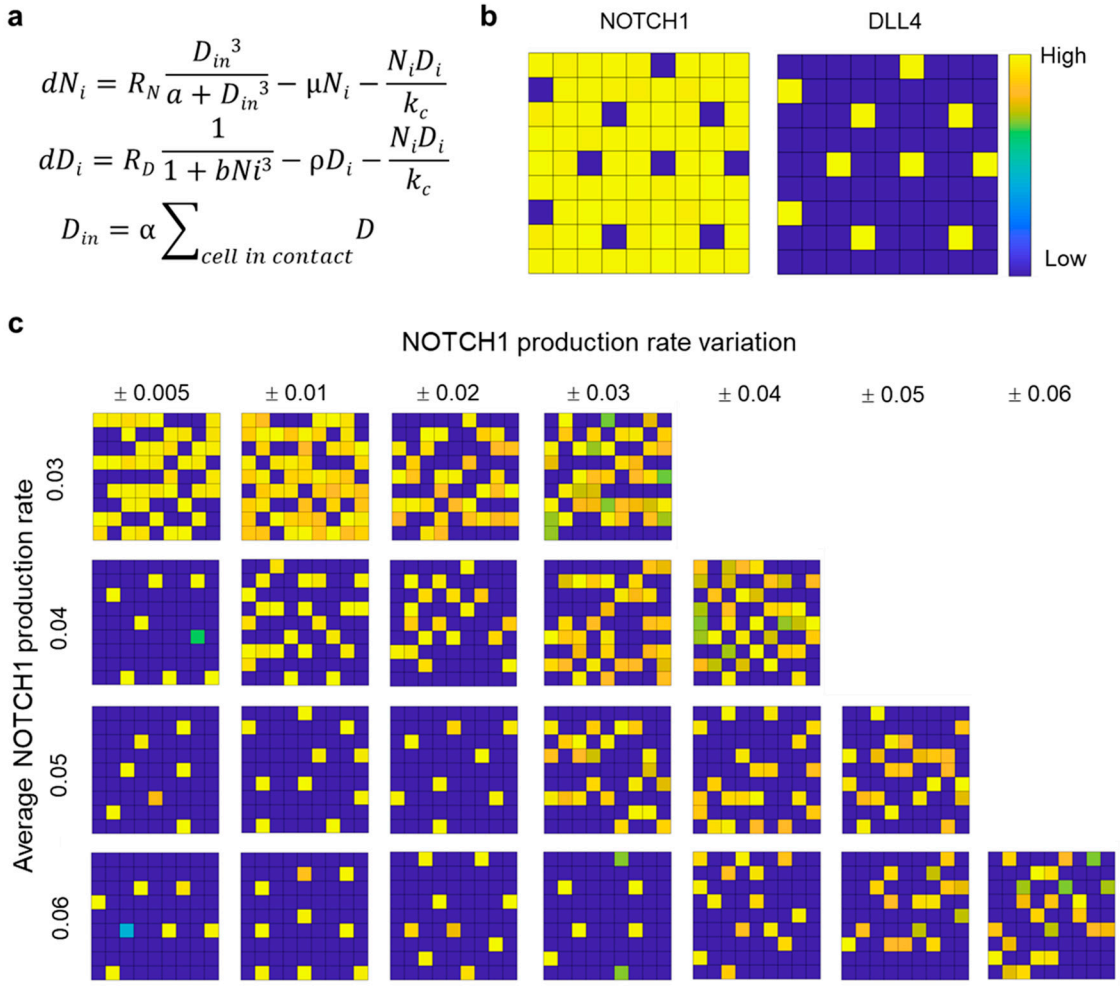

Figure 6. Agent-based computational modeling reveals NOTCH1 variation enhances DLL4 expression. (**a**) Differential equations employed in the agent-based computational model of NOTCH1-DLL4 expression. (**b**) Formation a checker box pattern of DLL4 expression with homogeneous NOTCH1 production. (**c**) Effects of increasing average NOTCH1 production rate and NOTCH1 variation on DLL4 expression within the microtumor. The gray scale indicates the expression of DLL4 in arbitrary units. Results are representative of five simulations.

4. Discussion

This study demonstrated a combination of tumor bioengineering, single cell analysis, and computational modeling for investigating the influence of intratumoral heterogeneity on cancer invasiveness. Single cell biosensors and agent-based computation modeling provide useful tools for measuring and analyzing intratumoral heterogeneity. CRISPR/Cas9 gene editing and siRNA gene knockdown approaches directly test the role of subtype master regulators and molecular mechanisms important for invasion. Importantly, the tumor bioengineering approach incorporates multiple layers of matrices representing bladder basement membrane and lamina propria. Matrigel and collagen matrices are commonly applied for mimicking the basement membrane and stromal ECM [42], and cancer cells can adopt various invasion modes depending on the microenvironment [43,44]. Our invasion model resolves the potential of cancer cells to breach the basement membrane matrix and then subsequently invade the lamina propria. The ability to cross both layers suggests that the cancer subtype, or the combination of cancer subtypes, has the potential to progress to the muscularis propria (i.e., muscle invasive), an important distinction in prognosis

and management of bladder cancer. Unlike models that mixed multiple matrices [45,46], the multilayer approach revealed microtumor subpopulations with distinct abilities of invading different matrices, as indicated by microtumors trapped at the Matrigel–collagen interface. Overall, the tumor bioengineering approach provides a useful platform for characterizing the influence of intratumoral heterogeneity in a bladder mimicking environment. Logical continuations of this work would include further development of a multilayer tissue model to include other important components, such as fibroblasts, macrophages, healthy urothelial cells, and microvasculature (or nutrient supply) and also incorporation of more cancer cell lines and combinations in the multilayer model. Additional molecular approaches should also be incorporated to rule out potential off-target effects and limitations of the experimental design.

Using the tumor bioengineering approach, our results revealed intratumoral heterogeneity can enhance the invasiveness of microtumors. The heterogeneity mediated invasiveness was demonstrated using cell lines with distinct patterns of luminal (FOXA1, PPARG, and GATA3) and basal (KRT5 and KRT14) markers (Supplementary Figure S10). For invasive cells (e.g., HT-1376), the invasion depth of individual microtumors was similar to mixed microtumors with both invasive and non-invasive cells (e.g., HT-1376 mixed with UM-UC-1). This observation is in analogous to a heterotypic co-culture model of breast cancer, in which invasive malignant cells induce collective invasion of non-invasive cells [13]. Distinctively, the combination of SCaBER and UM-UC-1 was striking because of the synergistic enhancement of invasiveness. Based on the invasive fraction, SCaBER and UM-UC-1 were actually the least invasive basal and luminal cell lines in this study. SCaBER and UM-UC-1 in co-culture showed much higher invasive potential than either cell line individually. When cultured separately, these cells exhibited only zero-to-low invasiveness in both single layer and multilayer models while combining the cell lines results in a large (>40%) invasive fraction. The mixed microtumor displayed an enhanced capability of breaching through both Matrigel and collagen matrices.

This study was motivated by the intratumoral heterogeneity associated with high-stage disease [10,11]. Our data revealed that NOTCH1-DLL4 signaling may play an important role in the heterogeneity induced invasiveness. In particular, the invasiveness of microtumors were enhanced by the intratumoral dissimilarity (or variation) of NOTCH1 expression, instead of the average expression. The NOTCH expressions of SCaBER and UM-UC-1 cells were determined by the GNR-LNA single cell biosensor, which measured the expression of the microtumor in the 3D environment. NOTCH1 expression was significantly higher in UM-UC-1 microtumors than in SCaBER or co-culture, and mixed microtumor exhibited a large variation of NOTCH expression. Furthermore, transient knockdown of NOTCH1 in either UM-UC-1 and SCaBER, which promoted heterogeneity, resulted in a large invasive fraction (~35%) while NOTCH1 knockdown in both cells reduced the fraction of cells progressed to the collagen layer. The view that variation of NOTCH1 contributes to the enhanced invasiveness of heterogeneous is further supported by CRISPR-Cas9 gene knockout of FOXA-1. FOXA-1 KO reduced NOTCH1 and NOTCH1 target genes. While CRISPR KO of FOXA1 in UM-UC-1 did not have a strong effect on its invasiveness, co-culture of wild-type and FOXA1 KO cells resulted in a clear increase in invasiveness. In particular, FOXA-1 KO itself did not lead to a large increase in invasiveness compared to the wild-type UM-UC-1 cells. On the other hand, the co-culture of UM-UC-1 and UM-UC-1 FOXA KO cells, which introduced a large variation in NOTCH1 expression within the microtumor, significantly enhanced the microtumor invasiveness.

Multiple mechanisms may contribute to the intratumoral heterogeneity mediated tumor invasiveness. For instance, co-culture models may modulate the growth and size of the microtumor. However, we did not observe a strong size effect in our model (Supplementary Figure S4). In contrast, our computational model revealed that intratumoral variation in NOTCH1 promoted the expression of DLL4 and formed clusters of DLL4 cells. In the experiment, DLL4 knockdown in UM-UC-1 and SCaBER reduced the invasive fraction into the collagen layer for both individual culture and co-culture. This supportive role of DLL4

in collective invasion is consistent with previous work examining NOTCH1-DLL4 signaling in HT-1376 bladder cancer cells and other cell models [19–22]. Nevertheless, DLL4 may not be the only factor that supports the collective invasion process. Other ligands of NOTCH signaling, such as JAG1, may also be involved in the collective invasion process. For instance, epigenetic heterogeneity and JAG1 signaling were recently shown to jointly promote the persistence of filopodia via the MYO10 in invading cancer cells [47]. The filopodia activity is necessary for creating migration tracks by micropatterning extracellular fibronectin in a 3D invasion model of Matrigel. Tumor heterogeneity, such as presence of luminal–basal and other molecular subtypes, may also enhance tumor invasiveness and survival capability via additional mechanisms.

There are several limitations of the study. In particular, the simplified computational model was not an explicit representation of the underlying signaling network [48], and the model parameters were not verified quantitatively. The computational model was only intended to illustrate the potential influence of NOTCH variation. Furthermore, the experimental data were based on cell lines. Physiologically relevant models (e.g., tumor organoids and animal models) and cancer patients with intratumor heterogeneity will be required to evaluate the clinical significance of the results. Thirdly, our data did not rule out the potential off target effect of the siRNA. Other specific ways of perturbing one or multiple genes (e.g., additional siRNA and CRIPSR/Cas9 gene editing) should be performed. Further investigation will be required to clarify the functions of NOTCH signaling in collective cancer invasion and examine other molecular processes associated with tumor heterogeneity.

Supplementary Materials: The following are available online at https://www.mdpi.com/article/10.3390/cells10113084/s1, Figure S1: Clustering analysis defines the invasive fraction of microtumors in the single layer invasion model. Figure S2: Co-culture enhances invasiveness of microtumors compared to individual cell lines. Figure S3: Comparison of invasion depth of mixed microtumors of luminal and basal cells. Figure S4: Size distributions of homogeneous and heterogeneous microtumors. Figure S5: SCaBER and UM-UC-1 invasion of Matrigel. Figure S6: Live cell biosensors for measuring NOTCH1 and DLL4 expression in 3D microtumors. Figure S7: Transient knockdown efficiency of NOTCH1 and DLL4 siRNA. Figure S8: Computation modeling of NOTCH1 and DLL4. Figure S9: Computation modeling of DLL4 expression with variation of NOTCH1 production rate. Figure S10: Comparison of cancer cell line encyclopedia RNA-seq data for luminal and basal cell lines. Table S1: Classification of cell lines based on the consensus classification of MIBC classifier. Table S2: Chi-square analysis and Fisher's exact test of data in Figure 2e. Table S3: Chi-square analysis and Fisher's exact test of data in Figure 4c. Table S4: Chi-square analysis and Fisher's exact test of data in Figure 4d. Table S5: Chi-square analysis and Fisher's exact test of data in Figure 5b. Movie S1: Heterogeneous microtumors in 3D microenvironment. Movie S2: Heterogeneous microtumors formed by bladder cancer cells of luminal papillary (UM-UC-1) and basal/squamous (SCaBER) subtypes. Movie S3: Heterogeneous microtumors formed by bladder cancer cells of luminal papillary (UM-UC-1) and basal/squamous (SCaBER) subtypes.

Author Contributions: Conceptualization, J.I.W., J.D.R., D.J.D. and P.K.W.; Data curation, P.T.; Formal analysis, P.T., Y.Y. and P.K.W.; Investigation, P.T. and P.K.W.; Resources, H.Y. and D.J.D. Software, P.T., M.A. and P.K.W. All authors have read and agreed to the published version of the manuscript.

Funding: This work is supported by NSF Biophotonics Program 1802947 (PW) and the Penn State Grace Woodward Grant (P.K.W., D.J.D., J.D.R.).

Institutional Review Board Statement: Not applicable.

Informed Consent Statement: Not applicable.

Data Availability Statement: All data are included in the article and supplementary material. Further inquiries can be directed to the corresponding authors.

Conflicts of Interest: The authors declare no conflict of interest.

References

1. Siegel, R.L.; Miller, K.D.; Fuchs, H.E.; Jemal, A. Cancer Statistics, 2021. *CA Cancer J. Clin.* **2021**, *71*, 7–33. [CrossRef]
2. Cancer Genome Atlas Research, N. Comprehensive molecular characterization of urothelial bladder carcinoma. *Nature* **2014**, *507*, 315–322. [CrossRef]
3. Choi, W.; Porten, S.; Kim, S.; Willis, D.; Plimack, E.R.; Hoffman-Censits, J.; Roth, B.; Cheng, T.; Tran, M.; Lee, I.L.; et al. Identification of distinct basal and luminal subtypes of muscle-invasive bladder cancer with different sensitivities to frontline chemotherapy. *Cancer Cell* **2014**, *25*, 152–165. [CrossRef] [PubMed]
4. Damrauer, J.S.; Hoadley, K.A.; Chism, D.D.; Fan, C.; Tiganelli, C.J.; Wobker, S.E.; Yeh, J.J.; Milowsky, M.I.; Iyer, G.; Parker, J.S.; et al. Intrinsic subtypes of high-grade bladder cancer reflect the hallmarks of breast cancer biology. *Proc. Natl. Acad. Sci. USA* **2014**, *111*, 3110–3115. [CrossRef] [PubMed]
5. Kamoun, A.; de Reynies, A.; Allory, Y.; Sjodahl, G.; Robertson, A.G.; Seiler, R.; Hoadley, K.A.; Groeneveld, C.S.; Al-Ahmadie, H.; Choi, W.; et al. A Consensus Molecular Classification of Muscle-invasive Bladder Cancer. *Eur. Urol.* **2020**, *77*, 420–433. [CrossRef]
6. Warrick, J.I.; Walter, V.; Yamashita, H.; Shuman, L.; Amponsa, V.O.; Zheng, Z.; Chan, W.; Whitcomb, T.L.; Yue, F.; Iyyanki, T.; et al. FOXA1, GATA3 and PPAR Cooperate to Drive Luminal Subtype in Bladder Cancer: A Molecular Analysis of Established Human Cell Lines. *Sci. Rep.* **2016**, *6*, 38531. [CrossRef]
7. Yamashita, H.; Kawasawa, Y.I.; Shuman, L.; Zheng, Z.; Tran, T.; Walter, V.; Warrick, J.I.; Chen, G.; Al-Ahmadie, H.; Kaag, M.; et al. Repression of transcription factor AP-2 alpha by PPARgamma reveals a novel transcriptional circuit in basal-squamous bladder cancer. *Oncogenesis* **2019**, *8*, 69. [CrossRef] [PubMed]
8. Mariathasan, S.; Turley, S.J.; Nickles, D.; Castiglioni, A.; Yuen, K.; Wang, Y.; Kadel, E.E., III; Koeppen, H.; Astarita, J.L.; Cubas, R.; et al. TGFbeta attenuates tumour response to PD-L1 blockade by contributing to exclusion of T cells. *Nature* **2018**, *554*, 544–548. [CrossRef]
9. McGranahan, N.; Swanton, C. Biological and therapeutic impact of intratumor heterogeneity in cancer evolution. *Cancer Cell* **2015**, *27*, 15–26. [CrossRef] [PubMed]
10. Liu, Y.; Bui, M.M.; Xu, B. Urothelial Carcinoma With Squamous Differentiation Is Associated With High Tumor Stage and Pelvic Lymph-Node Metastasis. *Cancer Control* **2017**, *24*, 78–82. [CrossRef] [PubMed]
11. Warrick, J.I.; Sjodahl, G.; Kaag, M.; Raman, J.D.; Merrill, S.; Shuman, L.; Chen, G.; Walter, V.; DeGraff, D.J. Intratumoral Heterogeneity of Bladder Cancer by Molecular Subtypes and Histologic Variants. *Eur. Urol.* **2019**, *75*, 18–22. [CrossRef] [PubMed]
12. Vilchez Mercedes, S.A.; Bocci, F.; Levine, H.; Onuchic, J.N.; Jolly, M.K.; Wong, P.K. Decoding leader cells in collective cancer invasion. *Nat. Rev. Cancer* **2021**, *21*, 592–604. [CrossRef]
13. Carey, S.P.; Starchenko, A.; McGregor, A.L.; Reinhart-King, C.A. Leading malignant cells initiate collective epithelial cell invasion in a three-dimensional heterotypic tumor spheroid model. *Clin. Exp. Metastasis* **2013**, *30*, 615–630. [CrossRef] [PubMed]
14. Cheung, K.J.; Gabrielson, E.; Werb, Z.; Ewald, A.J. Collective invasion in breast cancer requires a conserved basal epithelial program. *Cell* **2013**, *155*, 1639–1651. [CrossRef] [PubMed]
15. Hwang, P.Y.; Brenot, A.; King, A.C.; Longmore, G.D.; George, S.C. Randomly Distributed K14(+) Breast Tumor Cells Polarize to the Leading Edge and Guide Collective Migration in Response to Chemical and Mechanical Environmental Cues. *Cancer Res.* **2019**, *79*, 1899–1912. [CrossRef]
16. Rampias, T.; Vgenopoulou, P.; Avgeris, M.; Polyzos, A.; Stravodimos, K.; Valavanis, C.; Scorilas, A.; Klinakis, A. A new tumor suppressor role for the Notch pathway in bladder cancer. *Nat. Med.* **2014**, *20*, 1199–1205. [CrossRef] [PubMed]
17. Maraver, A.; Fernandez-Marcos, P.J.; Cash, T.P.; Mendez-Pertuz, M.; Duenas, M.; Maietta, P.; Martinelli, P.; Munoz-Martin, M.; Martinez-Fernandez, M.; Canamero, M.; et al. NOTCH pathway inactivation promotes bladder cancer progression. *J. Clin. Investig.* **2015**, *125*, 824–830. [CrossRef]
18. Goriki, A.; Seiler, R.; Wyatt, A.W.; Contreras-Sanz, A.; Bhat, A.; Matsubara, A.; Hayashi, T.; Black, P.C. Unravelling disparate roles of NOTCH in bladder cancer. *Nat. Rev. Urol.* **2018**, *15*, 345–357. [CrossRef]
19. Riahi, R.; Sun, J.; Wang, S.; Long, M.; Zhang, D.D.; Wong, P.K. Notch1-Dll4 signalling and mechanical force regulate leader cell formation during collective cell migration. *Nat. Commun.* **2015**, *6*, 6556. [CrossRef]
20. Dean, Z.S.; Elias, P.; Jamilpour, N.; Utzinger, U.; Wong, P.K. Probing 3D Collective Cancer Invasion Using Double-Stranded Locked Nucleic Acid Biosensors. *Anal. Chem.* **2016**, *88*, 8902–8907. [CrossRef]
21. Wang, K.; Fan, H.Y.; Pang, X.; Zhang, M.; Yu, X.H.; Wu, J.S.; Chen, B.J.; Jiang, J.; Liang, X.H.; Tang, Y.L. Dll4/Notch1 signalling pathway is required in collective invasion of salivary adenoid cystic carcinoma. *Oncol. Rep.* **2021**, *45*, 1011–1022. [CrossRef]
22. Torab, P.; Yan, Y.; Yamashita, H.; Warrick, J.I.; Raman, J.D.; DeGraff, D.J.; Wong, P.K. Three-Dimensional Microtumors for Probing Heterogeneity of Invasive Bladder Cancer. *Anal. Chem.* **2020**, *92*, 8768–8775. [CrossRef] [PubMed]
23. Roeder, B.A.; Kokini, K.; Sturgis, J.E.; Robinson, J.P.; Voytik-Harbin, S.L. Tensile mechanical properties of three-dimensional type I collagen extracellular matrices with varied microstructure. *J. Biomech Eng.* **2002**, *124*, 214–222. [CrossRef] [PubMed]
24. Doyle, A.D. Generation of 3D Collagen Gels with Controlled Diverse Architectures. *Curr. Protoc. Cell Biol.* **2016**, *72*, 10.20.1–10.20.16. [CrossRef] [PubMed]
25. Achilli, M.; Mantovani, D. Tailoring Mechanical Properties of Collagen-Based Scaffolds for Vascular Tissue Engineering: The Effects of pH, Temperature and Ionic Strength on Gelation. *Polymers* **2010**, *2*, 664–680. [CrossRef]
26. Xiao, Y.; Riahi, R.; Torab, P.; Zhang, D.D.; Wong, P.K. Collective Cell Migration in 3D Epithelial Wound Healing. *ACS Nano* **2019**, *13*, 1204–1212. [CrossRef] [PubMed]

27. Wan, Y.; Zhu, N.; Lu, Y.; Wong, P.K. DNA Transformer for Visualizing Endogenous RNA Dynamics in Live Cells. *Anal. Chem* **2019**, *91*, 2626–2633. [CrossRef]
28. Cohen, M.; Georgiou, M.; Stevenson, N.L.; Miodownik, M.; Baum, B. Dynamic Filopodia Transmit Intermittent Delta-Notch Signaling to Drive Pattern Refinement during Lateral Inhibition. *Dev. Cell* **2010**, *19*, 78–89. [CrossRef]
29. Zuiverloon, T.C.M.; de Jong, F.C.; Costello, J.C.; Theodorescu, D. Systematic Review: Characteristics and Preclinical Uses of Bladder Cancer Cell Lines. *Bladder Cancer* **2018**, *4*, 169–183. [CrossRef]
30. Luo, Y.; Zhu, Y.T.; Ma, L.L.; Pang, S.Y.; Wei, L.J.; Lei, C.Y.; He, C.W.; Tan, W.L. Characteristics of bladder transitional cell carcinoma with E-cadherin and N-cadherin double-negative expression. *Oncol. Lett.* **2016**, *12*, 530–536. [CrossRef]
31. Fujiyama, C.; Jones, A.; Fuggle, S.; Bicknell, R.; Cranston, D.; Harris, A.L. Human bladder cancer invasion model using rat bladder in vitro and its use to test mechanisms and therapeutic inhibitors of invasion. *Br. J. Cancer* **2001**, *84*, 558–564. [CrossRef]
32. Jager, W.; Moskalev, I.; Janssen, C.; Hayashi, T.; Gust, K.M.; Awrey, S.; Black, P.C. Minimally Invasive Establishment of Murine Orthotopic Bladder Xenografts. *Jove J. Vis. Exp.* **2014**, *84*, e51123. [CrossRef] [PubMed]
33. Style, R.W.; Hyland, C.; Boltyanskiy, R.; Wettlaufer, J.S.; Dufresne, E.R. Surface tension and contact with soft elastic solids. *Nat. Commun.* **2013**, *4*, 2728. [CrossRef] [PubMed]
34. Ramakrishnan, S.; Huss, W.; Foster, B.; Ohm, J.; Wang, J.; Azabdaftari, G.; Eng, K.H.; Woloszynska-Read, A. Transcriptional changes associated with in vivo growth of muscle-invasive bladder cancer cell lines in nude mice. *Am. J. Clin. Exp. Urol.* **2018**, *6*, 138–148.
35. Padmanaban, V.; Tsehay, Y.; Cheung, K.J.; Ewald, A.J.; Bader, J.S. Between-tumor and within-tumor heterogeneity in invasive potential. *PLoS Comput. Biol.* **2020**, *16*, e1007464. [CrossRef] [PubMed]
36. Wang, S.; Riahi, R.; Li, N.; Zhang, D.D.; Wong, P.K. Single Cell Nanobiosensors for Dynamic Gene Expression Profiling in Native Tissue Microenvironments. *Adv. Mater.* **2015**, *27*, 6034–6038. [CrossRef]
37. Tao, S.; Wang, S.; Moghaddam, S.J.; Ooi, A.; Chapman, E.; Wong, P.K.; Zhang, D.D. Oncogenic KRAS confers chemoresistance by upregulating NRF2. *Cancer Res.* **2014**, *74*, 7430–7441. [CrossRef]
38. Warrick, J.I.; Kaag, M.; Raman, J.D.; Chan, W.; Tran, T.; Kunchala, S.; Shuman, L.; DeGraff, D.; Chen, G. FOXA1 and CK14 as markers of luminal and basal subtypes in histologic variants of bladder cancer and their associated conventional urothelial carcinoma. *Virchows Arch. Int. J. Pathol.* **2017**, *471*, 337–345. [CrossRef]
39. Qiu, M.; Bao, W.; Wang, J.; Yang, T.; He, X.; Liao, Y.; Wan, X. FOXA1 promotes tumor cell proliferation through AR involving the Notch pathway in endometrial cancer. *BMC Cancer* **2014**, *14*, 78. [CrossRef]
40. Fortini, M.E. Notch Signaling: The Core Pathway and Its Posttranslational Regulation. *Dev. Cell* **2009**, *16*, 633–647. [CrossRef]
41. Shaya, O.; Sprinzak, D. From Notch signaling to fine-grained patterning: Modeling meets experiments. *Curr. Opin. Genet. Dev.* **2011**, *21*, 732–739. [CrossRef]
42. Nguyen-Ngoc, K.V.; Cheung, K.J.; Brenot, A.; Shamir, E.R.; Gray, R.S.; Hines, W.C.; Yaswen, P.; Werb, Z.; Ewald, A.J. ECM microenvironment regulates collective migration and local dissemination in normal and malignant mammary epithelium. *Proc. Natl. Acad. Sci. USA* **2012**, *109*, E2595–E2604. [CrossRef] [PubMed]
43. Clark, A.G.; Vignjevic, D.M. Modes of cancer cell invasion and the role of the microenvironment. *Curr. Opin. Cell Biol.* **2015**, *36*, 13–22. [CrossRef]
44. Friedl, P.; Locker, J.; Sahai, E.; Segall, J.E. Classifying collective cancer cell invasion. *Nat. Cell Biol.* **2012**, *14*, 777–783. [CrossRef]
45. Carey, S.P.; Martin, K.E.; Reinhart-King, C.A. Three-dimensional collagen matrix induces a mechanosensitive invasive epithelial phenotype. *Sci. Rep.* **2017**, *7*, 42088. [CrossRef]
46. Anguiano, M.; Morales, X.; Castilla, C.; Pena, A.R.; Ederra, C.; Martinez, M.; Ariz, M.; Esparza, M.; Amaveda, H.; Mora, M.; et al. The use of mixed collagen-Matrigel matrices of increasing complexity recapitulates the biphasic role of cell adhesion in cancer cell migration: ECM sensing, remodeling and forces at the leading edge of cancer invasion. *PLoS ONE* **2020**, *15*, e0220019. [CrossRef]
47. Summerbell, E.R.; Mouw, J.K.; Bell, J.S.K.; Knippler, C.M.; Pedro, B.; Arnst, J.L.; Khatib, T.O.; Commander, R.; Barwick, B.G.; Konen, J.; et al. Epigenetically heterogeneous tumor cells direct collective invasion through filopodia-driven fibronectin micropatterning. *Sci. Adv.* **2020**, *6*, eaaz6197. [CrossRef] [PubMed]
48. Vilchez Mercedes, S.A.; Bocci, F.; Zhu, N.; Levine, H.; Onuchic, J.N.; Jolly, M.K.; Wong, P.K. Nrf2 modulates the hybrid epithelial/mesenchymal phenotype and Notch signaling during collective cancer migration. *bioRxiv* **2021**, 2021-04. Available online: https://www.biorxiv.org/content/10.1101/2021.04.21.440858v2 (accessed on 10 September 2021). [CrossRef]